Syntheses and crystal structures of iron co-ordination polymers with 4,4′-bipyridine (4,4′-bpy) and 4,4′-azopyridine (azpy). Two-dimensional networks supported by hydrogen bonding, {[Fe(azpy)(NCS)$_2$(MeOH)$_2$]·azpy}$_n$ and {[Fe(4,4′-bpy)(NCS)$_2$-(H$_2$O)$_2$]·4,4′-bpy}$_n$

Shin-ichiro Noro,[a] Mitsuru Kondo,[b] Tomohiko Ishii,[a] Susumu Kitagawa *[b] and Hiroyuki Matsuzaka[a]

[a] Department of Chemistry, Graduate School of Science, Tokyo Metropolitan University, 1-1 Minamiohsawa, Hachioji-shi, Tokyo 192-0397, Japan
[b] Department of Synthetic Chemistry and Biological Chemistry, Graduate School of Engineering, Kyoto University, Yoshida, Sakyo-ku, Kyoto 606-8501, Japan

New iron(II) co-ordination polymers, {[Fe(azpy)(NCS)$_2$(MeOH)$_2$]·azpy}$_n$ 1 (azpy = 4,4′-azopyridine), {[Fe(4,4′-bpy)-(NCS)$_2$(H$_2$O)$_2$]·4,4′-bpy}$_n$ 2 (4,4′-bpy = 4,4′-bipyridine) and {[Fe(azpy)$_2$(NCS)$_2$]·3H$_2$O}$_n$ 3 have been synthesized and characterized. The crystal structures of both compounds 1 and 2 contain two types of bridging ligands; one is of the co-ordination bond type, directly bridging iron centers to form a one-dimensional chain of [Fe(L)] (L = azpy or 4,4′-bpy), while the other links these chains by hydrogen bonds between the pyridine nitrogen atoms and co-ordinated methanol or water molecules, resulting in a grid sheet. Each sheet shows non-interpenetration because of incorporation of NCS anion in the grid. Cyclic voltammograms of 1 and 3 demonstrate that the directly bridging azpy ligands show no apparent redox activity, whereas a reversible redox wave observed for 1 is attributed to the hydrogen-bonding supported azpy. Magnetic susceptibilities measured from 1.9 to 300 K are indicative of no appreciable magnetic exchange interaction between the adjacent metal ions.

Introduction

Square grid type sheets constructed from a metal ion with an octahedral environment and a rod-like bridging ligand are of great interest due to the versatility of the crystal structures, physical properties and catalytic reactivities.[1-12] Heterogeneous catalysis and spin cross-over behavior were observed in a two-dimensional channel structure of [Cd(4,4′-bpy)$_2$(NO$_3$)$_2$]$_n$[1] and a doubly interpenetrating network of [Fe{(4-NC$_5$H$_4$)CH=CH(4-NC$_5$H$_4$)}$_2$(NCS)$_2$]$_n$[10] respectively. As far as sheet structures with bipyridine derivatives are concerned, two types of networks are known (Scheme 1); type 1 is constructed from only co-ordination bonds, by which metal ions and ligands are directly linked, while type 2 consists of both co-ordination bonds for one-dimensional chains and hydrogen bonds for interchain links. Bridging ligands, pyrazine (pyz),[7,11,12] 4,4′-bpy[1,3,7-9] and 1,2-bis(4-pyridyl)ethylene,[10] afford type 1 structures, whose cavity shape is a square grid form. On the other hand, type 2, which provides a larger cavity size and non-square grid, dissimilar to type 1, has been restricted to the case of a 4,4′-bpy ligand.[2-6] We have chosen an azpy ligand as a building block for the construction of a new functional co-ordination network. It gives a longer metal–metal distance than that of 4,4′-bpy, and thus the type 2 co-ordination polymer affords a larger cavity size than those with 4,4′-bpy. Interestingly, azpy has a redox activity,[13] and a redox active co-ordination network is expected. Here we report the syntheses, crystal structures and redox properties of iron(II) co-ordination polymers with azpy and 4,4′-bpy.


4,4'-bpy   azpy
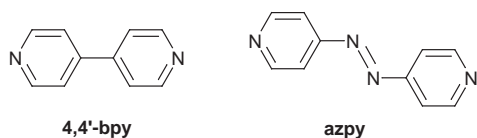
Experimental

Materials

The compounds Fe(ClO$_4$)$_2$·6H$_2$O and NH$_4$SCN were obtained from Aldrich Chemical Co. and Wako Co., respectively, 4,4′-bpy from Tokyo Kasei Chemical Co., azpy was prepared according to the literature method.[14,15]

Syntheses

{[Fe(azpy)(NCS)$_2$(MeOH)$_2$]·azpy}$_n$ 1. A methanol solution (20 mL) of azpy (0.75 g, 4.1 mmol) was added to a methanol solution (40 mL) containing a mixture of Fe(ClO$_4$)$_2$·6H$_2$O (0.75 g, 2.1 mmol) and NH$_4$SCN (0.31 g, 4.0 mmol). The black microcrystals were collected by filtration, washed with methanol, and dried *in vacuo* for 2 h. Yield: 1.03 g (1.70 mmol, 84%) (Found: C, 48.13; H, 4.09; N, 23.58. Calc. for C$_{24}$H$_{24}$FeN$_{10}$O$_2$S$_2$: C, 47.69; H, 4.00; N, 23.17%). IR (KBr pellet): 3399s, 2091s, 1639w, 1608m, 1597m, 1537w, 1489w, 1404w, 1215w, 1060w, 1059w, 1045w, 985w, 808m, 729w, 669w, 630m, 628m and 470w cm^{-1}.

After the microcrystals were collected, standing of the filtrate for a few weeks provided single crystals. One of these was used for single X-ray analysis. The homogeneity of the bulk product was confirmed by comparison of the observed and calculated powder diffraction patterns obtained from single crystal data.

{[Fe(4,4′-bpy)(NCS)$_2$(H$_2$O)$_2$]·4,4′-bpy}$_n$ 2. An ethanol solution (20 mL) containing 4,4′-bpy (0.64 g, 4.1 mmol) was added to an aqueous solution (20 mL) containing a mixture of Fe(ClO$_4$)$_2$·6H$_2$O (0.72 g, 2.0 mmol) and NH$_4$SCN (0.30 g, 3.9 mmol). The red powder was collected by filtration, washed with water and ethanol, and dried *in vacuo* for 2 h. Yield: 0.78 g (1.48

type 1

type 2
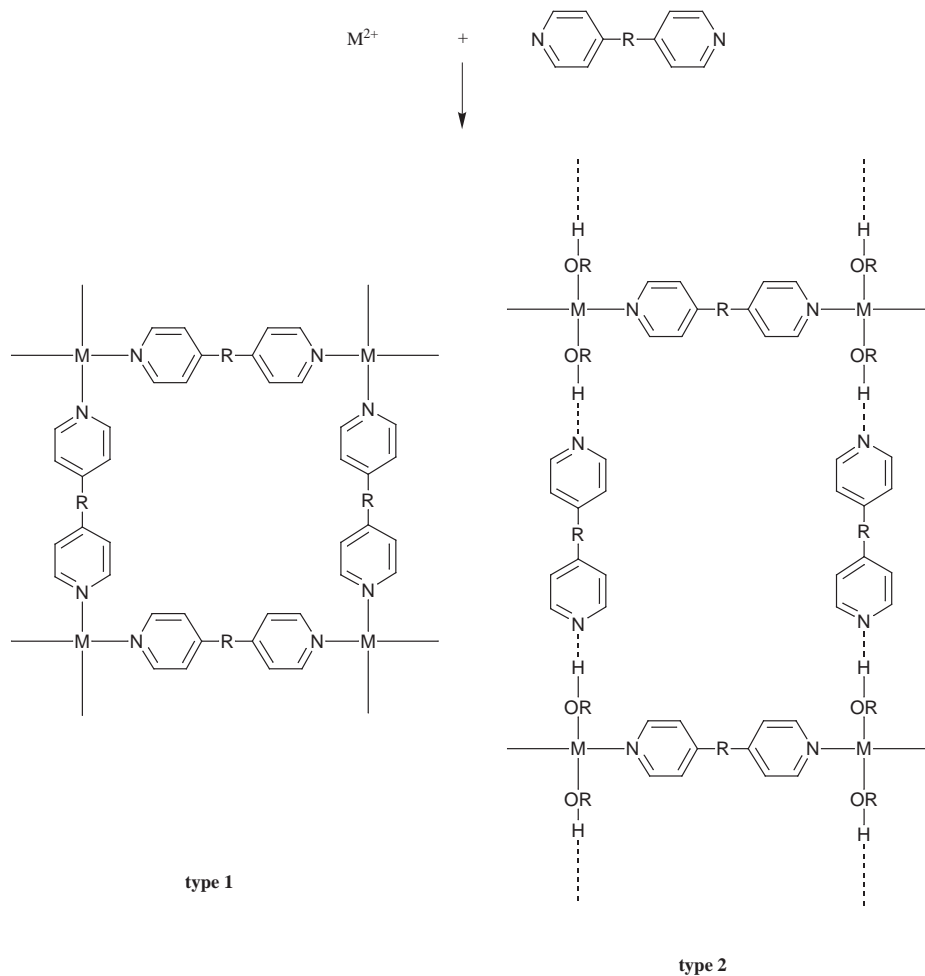
Scheme 1

mmol, 74%) (Found: C, 50.79; H, 3.75; N, 16.05. Calc. for $C_{22}H_{20}FeN_6O_2S_2$: C, 50.77; H, 3.87; N, 16.15%). IR (KBr pellet): 2988w, 2735w, 2546w, 2100m, 2075s, 2046s, 1599s, 1566w, 1414s, 1224w, 1049w, 1020m, 1008m, 848m, 839m, 572m, 544w and 524w cm^{-1}.

Single crystals suitable for X-ray analysis were prepared by the careful diffusion of an ethanol solution of 4,4′-bpy into an aqueous solution containing Fe(ClO$_4$)$_2$·6H$_2$O and NH$_4$SCN. The homogeneity of the bulk product was confirmed by comparison of the observed and calculated powder diffraction patterns obtained from single crystal data.

{[Fe(azpy)$_2$(NCS)$_2$]·3H$_2$O}$_n$ 3. A diethyl ether solution (20 mL) of azpy (0.050 g, 0.27 mmol) was added to a mixture of acetone (10 ml) and ethanol (10 ml) containing Fe(ClO$_4$)$_2$·6H$_2$O (0.049 g, 0.14 mmol) and NH$_4$SCN (0.020 g, 0.27 mmol). The dark purple powder was collected by filtration, washed with diethyl ether, acetone and ethanol, and dried *in vacuo* for 2 h. Yield: 0.052 g (0.09 mmol, 64%) (Found: C, 44.40; H, 3.76; N, 24.30. Calc. for $C_{22}H_{22}FeN_{10}O_3S_2$: C, 44.45; H, 3.73; N, 23.56%). IR (KBr pellet): 2102s, 2046s, 1637w, 1599m, 1566w, 1520w, 1489w, 1414m, 1223w, 1194w, 1049w, 1012w, 844m, 569m and 528w cm^{-1}.

Physical measurements

Elemental analyses were taken on a Yanaco C,H,N Corder MT-5 instrument. The IR spectra were recorded on a Hitachi I-5040FT-IR spectrometer with samples prepared as KBr pellets. X-Ray powder diffraction data were collected on a MAC Science MXP18 automated diffractometer by using Cu-Kα radiation. Thermal gravimetric (TG) analyses were carried out with a Seiko Instruments SSC5200 instrument in a nitrogen atmosphere (heating rate: 5 K min^{-1}).

The cyclic voltammograms were taken on a BAS CV-50W polarographic analyzer. A SCE electrode was used as a reference. Each bulk sample of compounds **1**, **2** and **3** was added to carbon paste (graphite and mineral oil) and mixed well. By using this mixture a working electrode was prepared; the mixture was set in a cavity on a Teflon rod, connected to a platinum wire. Another platinum wire was used as a counter electrode. Three-electrode systems were employed in 0.1 mol dm^{-3} NaClO$_4$ aqueous solution, using a scan rate of 10 mV s^{-1} in the range from −1.2 to 1.2 V.

Crystal structure determination

A single crystal of each compound **1** and **2** was sealed in a glass capillary. X-Ray data collections were carried out by an oscillation method using a Rigaku R-AXIS IV imaging-plate system on a rotating-anode X-ray generator operated at 50 kV and 100 mA. Laue group and unit-cell parameters were determined by data-processing software (PROCESS) attached to the R-AXIS system. Lorentz-polarization corrections were applied. For **1**, the structure was solved by a direct method using the SHELXS 86 program[16] and expanded using Fourier techniques.[17] The non-hydrogen atoms were refined anisotropically. All hydrogen atoms, which were placed in idealized positions, were included but not refined. The refinements were carried out using full-matrix least squares techniques. For **2**, the structure was solved by a direct method using the SIR 92 program[18] and expanded using Fourier techniques.[17] The non-hydrogen atoms were refined anisotropically. All hydrogen atoms, which were placed in idealized positions, were included but not refined. The
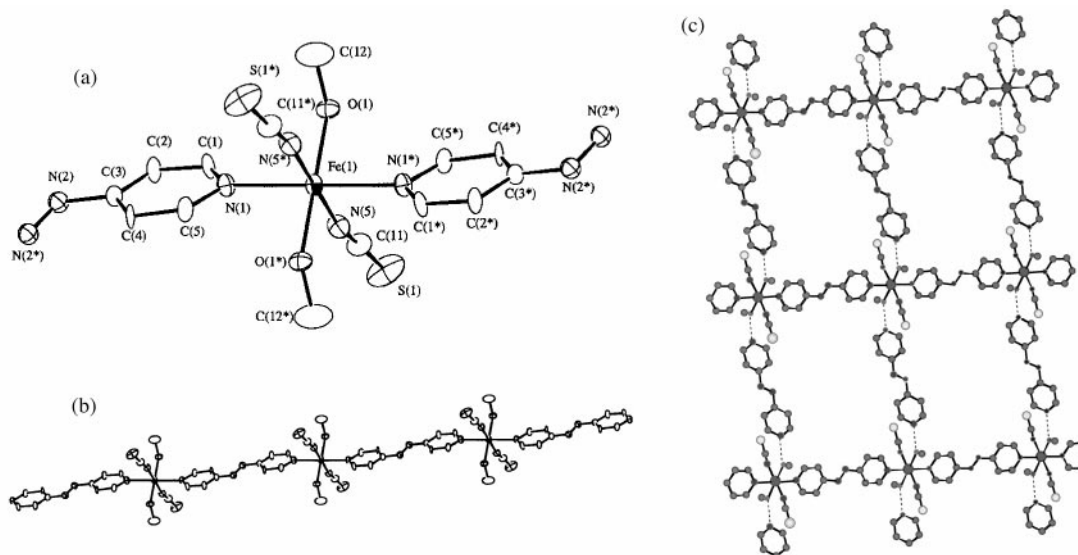
Fig. 1 (a) An ORTEP drawing of an iron center of compound **1** at the 30% probability level. (b) An ORTEP drawing of an infinite one-dimensional chain at the 30% probability level. (c) View of a sheet. Broken lines indicate hydrogen bonding.

Table 1 Crystallographic data for {[Fe(azpy)(NCS)₂(CH₃OH)₂]· azpy}$_n$ **1** and {[Fe(4,4′-bpy)(NCS)₂(H₂O)₂]·4,4′-bpy}$_n$ **2**

	1	**2**
Formula	$C_{24}H_{24}FeN_{10}O_2S_2$	$C_{22}H_{20}FeN_6O_2S_2$
Formula weight	604.49	520.41
Crystal system	Monoclinic	Triclinic
Space group	$P2_1/c$ (no. 14)	$P\bar{1}$ (no. 2)
$a/$Å	7.232(4)	9.017(1)
$b/$Å	16.960(3)	10.222(1)
$c/$Å	11.950(3)	7.489(1)
$\alpha/°$		104.318(9)
$\beta/°$	94.65(3)	96.65(1)
$\gamma/°$		107.454(10)
$V/$Å³	1460.9(7)	624.5(2)
Z	2	1
μ(Mo-Kα)/cm⁻¹	6.99	8.00
$T/°$C	23	23
R	0.063	0.047
R'	0.064	0.054
Reflections measured	2004	1962
Independent reflections	1168	1580

refinements were carried out using full-matrix least squares techniques. All calculations were performed using the TEXSAN crystallographic software package.[19] Crystal data are given in Table 1.

CCDC reference number 186/1389.

See http://www.rsc.org/suppdata/dt/1999/1569/ for crystallographic files in .cif format.

Results and discussion

Crystal structures

An ORTEP[20] view of an iron center of compound **1** is shown in Fig. 1(a) with numbering scheme, where the metal sites are on crystallographic inversion centers. Selected bond distances and angles are listed in Table 2(a). The iron has a distorted elongated octahedral environment with two thiocyanate nitrogen donors and two methanol molecules in the basal plane, and two pyridine nitrogen donors in the axial sites. Each ligand occupies the *trans* position. The *trans* N–Fe–N (NCS), N–Fe–N (py), and O–Fe–O bond angles are crystallographically 180°. On the other hand, *cis* N–Fe–O and N–Fe–N bond angles range from 85.9(2) to 91.1(3)° [Table 2(a)], indicative of a distorted octahedral environment. The NCS ligands are co-ordinated to the Fe atom in a bent fashion with the angle Fe(1)–N(5)–C(11)

Table 2 Selected bond distances (Å) and angles (°) for (a) {[Fe(azpy)-(NCS)₂(CH₃OH)₂]·azpy}$_n$ **1** and (b) {[Fe(4,4′-bpy)(NCS)₂(H₂O)₂]·4,4′-bpy}$_n$ **2**

(a) {[Fe(azpy)(NCS)₂(CH₃OH)₂]·azpy}$_n$ **1**

Fe(1)–O(1)	2.143(6)	N(5)–C(11)	1.156(10)
Fe(1)–N(1)	2.217(5)	S(1)–C(11)	1.616(9)
Fe(1)–N(5)	2.121(7)	O(1)–N(3*)	2.685(9)
O(1)–Fe(1)–N(1)	89.9(2)	O(1)–Fe(1)–N(5)	85.9(2)
N(1)–Fe(1)–N(5)	91.1(3)	Fe(1)–O(1)–C(12)	129.0(5)
Fe(1)–N(5)–C(11)	169.8(7)	S(1)–C(11)–N(5)	177.9(8)

Symmetry code: (*) $-x, \frac{1}{2} + y, \frac{1}{2} - z$.

(b) {[Fe(4,4′-bpy)(NCS)₂(H₂O)₂]·4,4′-bpy}$_n$ **2** ^{a}

Fe(1)–O(1)	2.135(4)	N(3)–C(11)	1.146(5)
Fe(1)–N(1)	2.216(3)	S(1)–C(11)	1.638(5)
Fe(1)–N(3)	2.134(4)	O(1)–N(2*)	2.725(5)
O(1)–Fe(1)–N(1)	89.9(1)	O(1)–Fe(1)–N(3)	89.8(2)
N(1)–Fe(1)–N(3)	89.3(1)	Fe(1)–N(3)–C(11)	168.0(4)
S(1)–C(11)–N(3)	178.0(4)		

Symmetry code: (*) $1 - x, -y, -z$. ^{a} The numbering schemes for 4,4′-bpy and NCS in compound **2** are similar to those of **1**. The oxygen atoms in **2** also have numbers corresponding to those of the methanol oxygen atoms in **1**.

of 169.8(7)°. The NCS ligand itself is almost linear, N(5)–C(11)–S(1) 177.9(8)°. The Fe(1)–O(1)–C(12) (CH₃OH) bond angle is 129.0(5)°.

All azpy ligands show a *trans* form. There are two types of association for the azpy ligand in the crystal. One is a co-ordination type, which shows direct bridging between the iron centers to form zigzag Fe–azpy–Fe chains [Fig. 1(b)] with the Fe···Fe separation of 13.46 Å. The other is a hydrogen bonding type and bridges the co-ordinated CH₃OH molecules in the nearest neighbor chains to form a Fe–(HOCH₃)–azpy–(CH₃OH)–Fe link [O(CH₃OH)–N(py) 2.685(9) Å]. The interchain distance of the Fe···Fe pair is 16.96 Å. The zigzag chain of Fe–(HOCH₃)–azpy–(CH₃OH)–Fe affords a stepwise two-dimensional structure having a polyhedral-type grid [Fig. 1(c)].

The structure of compound **2** is similar to that of analogs of Co and Mn with type 2 framework.[2,3] Selected bond distances and angles are listed in Table 2(b). The Fe has an elongated octahedral environment with two thiocyanate nitrogen donors and two water ligands in the equatorial positions, and two pyridine nitrogen donors in the axial positions. The Fe–N

(py), Fe–N (NCS) and Fe–O bond distances [2.216(3), 2.134(4) and 2.135(4) Å, respectively] are shorter than those of the manganese compound (average 2.278, 2.175 and 2.198 Å, respectively)[2] and longer than those of the cobalt compound [2.162(2), 2.095(2) and 2.096(2) Å, respectively].[3] These results are expected from the metal ion radii (Mn^{2+}, 0.970; Fe^{2+}, 0.920; and Co^{2+}, 0.885 Å). There are two types of association modes for the 4,4′-bpy ligand in the crystal as in **1**. One is a co-ordination bridge between the iron centers to form linear Fe–(4,4′-bpy)–Fe chains. The other is a hydrogen bonding type and bridges the co-ordinated H$_2$O molecules in the nearest neighbor chains. The sheets also show a stepwise two-dimensional structure of rectangular grids.

Both compounds **1** and **2** afford a sheet composed of poly-hedral- and rectangular-shaped grids, respectively, resulting in crystals with micro cavities of *ca.* 13.5 × 17.0 and *ca.* 11.5 × 15.8 Å, respectively, larger than those of type 1 of co-ordination polymers solely co-ordinated by 4,4′-bpy (*ca.* 11.5 × 11.5 Å).[1,3,8] Co-ordination polymers with 4,4′-bpy show-ing type 2 structure[2–6] have a channel shape (rectangular) and size (*ca.* 11.5 × 15.8 Å), similar to that of **2**. On the other hand, complex **1** forms a unique stepwise two-dimensional structure having a polyhedral-type grid [Fig. 1(c)], resulting from a link-age of azpy in a stepwise fashion. The cavities defined by four iron centers in the sheet have a size of *ca.* 13.5 × 17.0 Å, which is larger than those of **2** and the co-ordination polymers having similar type 2 structure (*ca.* 11.5 × 15.8 Å).[2–6] Complex **1** is the first example in which methanol molecules are involved in hydrogen-bonding links instead of water molecules for a type 2 structure. It is to be noted that **1** and **2** show non-interpenetrating networks regardless of the presence of the large cavities. This is because each grid in a layer is occupied by an NCS anion provided by the adjacent layer. A similar structural aspect has been found for the 4,4′-bpy complex {[Cu(4,4′-bpy)(BF$_4$)$_2$(H$_2$O)$_2$]·4,4′-bpy}$_n$.[5]

The crystal structure of compound **1** is comprised of two types of sheets, which are related to each other by the glide plane symmetry, leading to alternative stacks of these different sheets as demonstrated in Fig. 2(a). The two pyridine rings of the azpy ligands are constrained by the symmetry of the crystal to be coplanar, and alternate π stacks for A and B types of the azpy ligand are obtained, the separation being about 3.29 Å. The Fe in an adjacent layer lies above or below the center of the polyhedral-type grid. The shortest Fe · · · Fe separation between the nearest-neighbor sheets is 10.37 Å. In **2** there is only one type of sheet in the crystal as shown in Fig. 2(b). The two pyridine rings of 4,4′-bpy ligands are con-strained by the symmetry of the crystal to be coplanar, and alternate π stacks for A and B types of the 4,4′-bpy ligand are obtained, the separation being about 3.43 Å. The Fe in an adjacent layer lies above or below the center of this rectangle. The shortest Fe · · · Fe separation between the sheets is 9.07 Å. A similar stacking form of the sheet is found in {[Cu(4,4′-bpy)-(BF$_4$)$_2$(H$_2$O)$_2$]·4,4′-bpy}$_n$.[5] In the network of **2**, co-ordinated (A) and hydrogen-bonded (B) 4,4′-bpy ligands in the sheet are arranged in a parallel fashion, while the molecular plane of the corresponding azpy ligands of **1** show a dihedral angle of 26°.

Magnetic and thermal properties

The magnetic susceptibilities of compounds **1** and **2** as a func-tion of temperature (1.9–300 K) were measured. The temper-ature dependence of the magnetic susceptibilities obeys the Curie–Weiss law: $\chi_m = C/(T - \theta)$ (where C = 3.11 emu K mol^{-1} and θ = 0 K in **1**, C = 2.62 emu K mol^{-1} and θ = 0 K in **2**). Thus, there is practically no magnetic interaction between the neigh-boring iron(II) ions through the 4,4′-bpy or azpy bridges. A weak temperature dependence at low temperature of the magnetic moments is observed for both complexes due to the spin–orbit interaction, exhibiting maxima at about 28 and
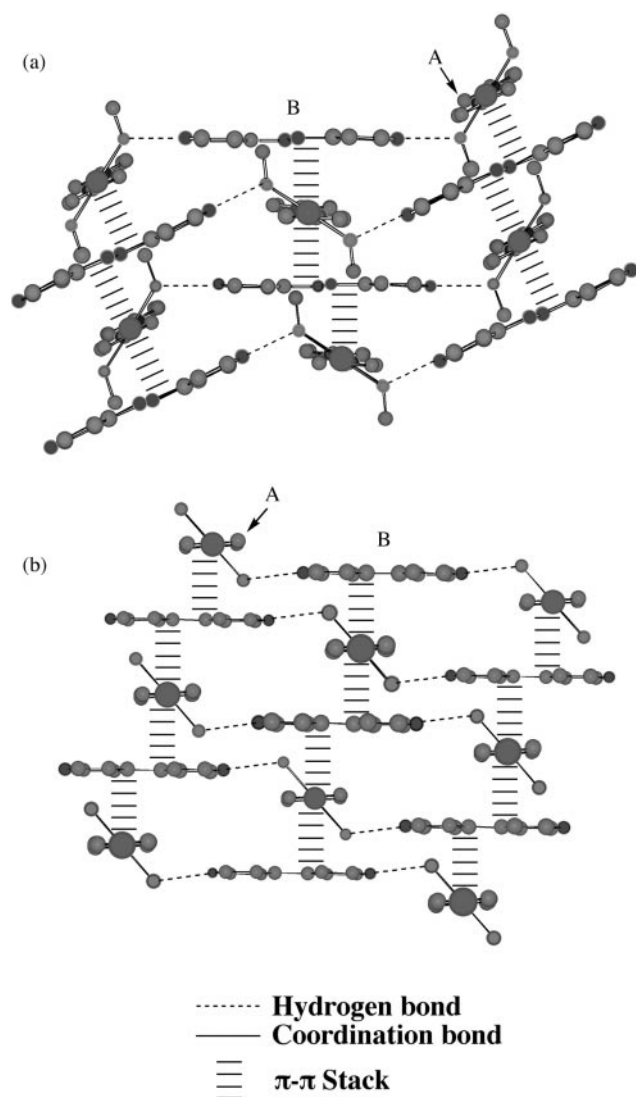

Fig. 2 View of the stacking forms of the sheets in (a) compound **1** and (b) **2**; the NCS anions are omitted for clarity.

15 K for **1** and **2**, respectively, where the moment can be estimated to be 4.90 μ_B (S = 2) only in the case of the absence of the spin–orbit interaction.

The thermal decomposition behaviors of compounds **1** and **2** are very similar to that reported for {[Mn(4,4′-bpy)(NCS)$_2$-(H$_2$O)$_2$]·4,4′-bpy}$_n$[2] and {[Co(4,4′-bpy)(NCS)$_2$(H$_2$O)$_2$]·4,4′-bpy}$_n$.[3] They were heated to 500 °C in N$_2$. The TGA data for **1** showed two steps of weight loss. In the first region 80–110 °C it loses two methanol molecules (observed 11.95, calculated 10.60%). On further heating, it loses one azpy ligand (observed 29.09, calculated 30.47%) between 150 and 200 °C, immediately followed by the other azpy ligand and decomposition of Fe(NCS)$_2$ above 210 °C. The weight loss continued up to 300 °C, and the final residue was black and amorphous. The TGA data for **2** showed two steps of weight loss. In the first region 80–110 °C it loses two water molecules (observed 7.02, calculated 6.92%). On further heating, it loses one 4,4′-bpy ligand (observed 29.23, calculated 30.01%) between 150 and 200 °C, immediately followed by the other 4,4′-bpy ligand and decomposition of Fe(NCS)$_2$ above 210 °C. The weight loss continued up to 300 °C, and the final residue was black and amorphous. All TGA data reveal that the methanol or water molecules are readily liberated from the iron(II) ion and the hydrogen bonded networks may be more brittle than co-ordination bonded networks. Consequently, the co-ordination networks with hydrogen bonded linkages afford flexible struc-tures and retain the electrochemical activity of the azpy.
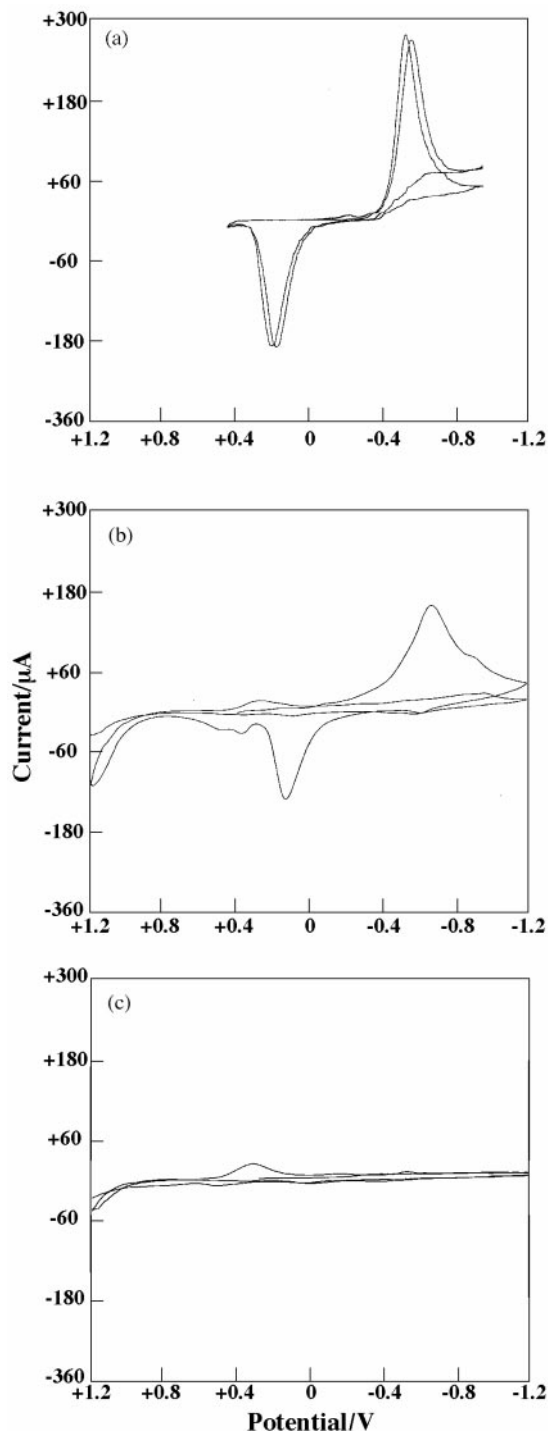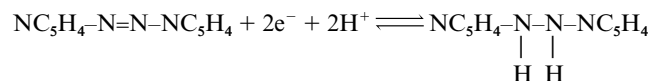
Fig. 3 Cyclic voltammograms of (a) free azpy, (b) compound **1**, and (c) **3** in carbon paste. Details of the measurements are mentioned in the text.

Redox properties

The electrochemical behavior of compounds **1**, **2** and **3** was were characterized by the measurement of the cyclic voltammograms in the solid state. One of the unique characteristics of azo-type compounds is the redox properties.[13] The electrochemical behavior of azpy, which depends on the properties of the solution, has been hitherto studied. It is reduced in two monoelectronic steps in DMF or acetonitrile solutions,[21,22] providing two coupled waves ($E_{1/2} = -0.84$ and -1.58 V vs. SCE in DMF, -1.67 and -2.29 V in acetonitrile). On the other hand, azpy in an aqueous buffer solution (pH 7) undergoes a reversible two-electron reduction,[13] which appears as a single coupled wave ($E_{1/2} = -0.13$ V vs. SCE for a gold electrode, -0.07 V for a

Metrohm hanging mercury drop electrode). These results show that a single coupled wave is observed when a proton donor coexists.

Measurements of cyclic voltammograms in the solid state were carried out by using the carbon paste method. Free azpy diluted in carbon paste shows a single coupled wave ($E_{p,c} = -0.61$ V, $E_{p,a} = 0.14$ V vs. SCE, $\Delta E = 0.75$ V), as shown in Fig. 3(a). This one-step reduction process is similar to that of azpy observed in aqueous buffer solution, based on the following mechanism.

$$NC_5H_4-N{=}N-NC_5H_4 + 2e^- + 2H^+ \rightleftharpoons NC_5H_4-\underset{\underset{H}{|}}{N}-\underset{\underset{H}{|}}{N}-NC_5H_4$$

The cyclic voltammogram of compound **1** in the solid state shows similar behavior to that of free azpy, as shown in Fig. 3(a) and (b) ($E_{p,c} = -0.66$ V and $E_{p,a} = 0.13$ V vs. SCE, $\Delta E = 0.79$ V). Compound **1** contains two types of azpy ligands; one directly links to Fe^{II}, the other contacts Fe^{II} through hydrogen bonding. On the other hand, we have also synthesized the co-ordination polymer $\{[Fe(azpy)_2(NCS)_2]\cdot 3H_2O\}_n$ **3**, which consists of a type 1 sheet (Scheme 1) with iron(II) ions and azpy at each corner and side, respectively.† The iron(II) atom has octahedral geometry with four pyridyl groups at the basal plane and two thiocyanate nitrogen atoms at the axial positions. This compound contains only one type of azpy ligand characteristic of co-ordination bonding.

In order to understand the redox properties of the azpy ligands contained in compound **1**, the cyclic voltammogram of **3** was measured under the same conditions and is shown in Fig. 3(c). In contrast to the case of **1**, **3** shows no redox waves between -1.2 and 1.2 V, indicative of no apparent redox activity of the co-ordination type azpy ligands. This result demonstrates that the clear reversible redox wave observed for **1** is attributed to the hydrogen-bonding supported azpy, while there is no activity for directly bridging azpy.

Conclusion

Three novel co-ordination polymers formed by Fe(ClO$_4$)$_2$·6H$_2$O and NH$_4$SCN with the bridging ligands 4,4′-bpy and azpy have been prepared and characterized: $\{[Fe(azpy)(NCS)_2(MeOH)_2]\cdot azpy\}_n$ **1** and $\{[Fe(4,4'-bpy)(NCS)_2(H_2O)_2]\cdot 4,4'-bpy\}_n$ **2** afford two-dimensional sheets supported by co-ordination and hydrogen bonds. Especially, complex **1** is the first example in which methanol molecules are involved in hydrogen-bonding links instead of water molecules for a type 2 structure (defined in Scheme 1). Both complexes show non-interpenetration regardless of the large cavities, since the NCS anions occupy these cavities.

The azpy ligand has unique redox properties.[13] Compound **1** contains two types of azpy ligands; one directly links to iron, the other contacts iron through hydrogen bonding. On the other hand, $\{[Fe(azpy)_2(NCS)_2]\cdot 3H_2O\}_n$ **3** contains only one type of azpy ligand, which is directly co-ordinated to the iron(II) ions. Cyclic voltammograms of **1** and **3** demonstrate that the

---

directly bridging azpy ligands show no apparent redox activity and a reversible redox wave observed for **1** is attributed to the hydrogen-bonding supported azpy.

In this paper we demonstrate that the azpy ligand is a suitable candidate for the design and construction of new co-ordination polymers having large polyhedral-shaped grids and redox active sites.

Acknowledgements

References

1 M. Fujita, Y. J. Kwon, S. Washizu and K. Ogura, *J. Am. Chem. Soc.*, 1994, **116**, 1151.
2 M. Li, G. Y. Xie and Y. D. Gu, *Polyhedron*, 1995, **14**, 1235.
3 J. Lu, T. Paliwala, S. C. Lim, C. Yu, T. Niu and A. J. Jacobson, *Inorg. Chem.*, 1997, **36**, 923.
4 L. Carlucci, G. Ciani, D. M. Proserpio and A. Sironi, *J. Chem. Soc., Dalton Trans.*, 1997, 1801.
5 A. J. Blake, S. J. Hill, P. Hubberstey and W. S. Li, *J. Chem. Soc., Dalton Trans.*, 1997, 913.
6 X. M. Chen, M. L. Tong, Y. J. Luo and Z. N. Chen, *Aust. J. Chem.*, 1996, **49**, 835.
7 M. L. Tong, X. M. Chen, X. L. Yu and T. C. W. Mak, *J. Chem. Soc., Dalton Trans.*, 1998, 5.
8 R. W. Gable, B. F. Hoskins and R. Robson, *J. Chem. Soc., Chem. Commun.*, 1990, 1667.
9 L. R. MacGillivary, R. H. Groeneman and J. L. Atwood, *J. Am. Chem. Soc.*, 1998, **120**, 2676.
10 J. A. Real, E. Andres, M. C. Munoz, M. Julve, T. Granier, A. Bousseksou and F. Varret, *Science*, 1995, **268**, 265.
11 J. A. Real, G. D. Munno, M. C. Munoz and M. Julve, *Inorg. Chem.*, 1991, **30**, 2071.
12 S. Kawata, S. Kitagawa, M. Kondo, I. Furuchi and M. Munakata, *Angew. Chem., Int. Ed. Engl.*, 1994, **33**, 1759.
13 J. Haladjian, R. Pilard, P. Bianco and L. Asso, *Electrochim. Acta*, 1985, **30**, 695.
14 E. V. Brown and G. R. Granneman, *J. Am. Chem. Soc.*, 1975, **97**, 621.
15 N. Campbell, A. W. Henderson and D. Taylor, *J. Chem. Soc.*, 1953, 1281.
16 G. M. Sheldrick, in *Crystallographic Computing 3*, eds. G. M. Sheldrick, C. Kruger and R. Goddard, Oxford University Press, 1985, pp. 175–189.
17 P. T. Beurskens, G. Admiraal, G. Beurskens, W. P. Bosman, S. Garcia-Granda, R. O. Gould, J. M. M. Smits and C. Smykalla, The DIRDIF Program System, Technical Report, Crystallography Laboratory, University of Nijmegen, 1992.
18 A. Altomare, M. C. Burla, M. Camalli, M. Cascarano, C. Giacovazzo, A. Guagliardi and G. Polidori, *J. Appl. Crystallogr.*, 1994, **27**, 435.
19 TEXSAN, TEXRAY Structure Analysis Package, Molecular Structure Corporation, The Woodlands, TX, 1985 and 1992.
20 C. K. Johnson, ORTEP II, Report ORNL-5138, Oak Ridge National Laboratory, TN, 1976.
21 J. L. Sadler and A. J. Bard, *J. Am. Chem. Soc.*, 1968, **90**, 1979.
22 A. J. Bellamy, I. S. MacKirdy and C. E. Niven, *J. Chem. Soc., Perkin Trans. 2*, 1983, 183.

Paper 8/09523J